Impact of Communication Erasure Channels on Control Performance of Connected and Automated Vehicles

Thu Nguyen, Le Yi Wang, George Yin, Hongwei Zhang, Shengbo Eben Li, Keqiang Li

***Abstract*—Connected and automated vehicles mandate integrated design of communications and control to achieve coordination of highway vehicles. Random features of wireless communications introduce new types of uncertainties into networked systems and impact control performance significantly. Due to typical packet loss, erasure channels create random link interruption and switching in network topologies. This paper models such switching network topologies by Markov chains and derives their probability transition matrices from stochastic characterizations of the channels. Impact of communication erasure channels on vehicle platoon formation and robustness under a weighted and constrained consensus framework is analyzed. By comparing convergence properties of networked control algorithms under different communication channel features, we characterize some intrinsic relationships between packet delivery ratio and convergence rate. Simulation case studies are performed to verify the theoretical findings.**

Keywords. Communications, erasure channel, platoon formation, networked system, consensus control.

I. Introduction

CONNECTED and automated vehicles (CAVs) coordinate highway vehicle operations by integrated network control, sensing, and communications [1], [2]. CAVs offer potential benefits of enhanced safety, more efficient highway usage, reduced fuel consumption, and improved passenger comfort. Vehicle platoons, as a fundamental framework of CAVs, have especially drawn great attention. During the past several decades, platoon control has been advanced extensively in methodology development, demonstration systems, and highway testing. These include platoon demonstration projects DEMO2000, CarTALK2000, FleetNet, PATH, AHS, and SARTRE [1], [3], [4]. Platoon formation, stability, robustness, reliability, operational complexity, and validations have been studied extensively, mostly in longitude operations, including decentralized control in [5], string stability of connected vehicles [6], and stability and robustness under adaptive cruise control [7], [8], to cite only a few. More complicated lane changes were investigated in [9]. Impact of sensor limitations was studied in [10]. Different control techniques such as adaptive observers [11], adaptive predictive control [12], and different feedback strategies [13] have been reported. [14] contains a comprehensive review of different network topologies and control strategies in platoon control.

Although direct sensor measurements by Radar, Lidar, or camera systems have already been deployed in commercial vehicles [15], wireless communication systems will be the main backbone platform for vehicle-to-vehicle communications in CAVs [16], [17]. At present, CAV connectivity is typically implemented by using the IEEE 802.11p-based Dedicated Short Range Communications (DSRC) or cellular networks (e.g., LTE and 5G). Analytical models of reliability of the IEEE 802.11p in VANET's safety [18] and performance evaluations of safety in the DSRC networks have been studied in [17].

Random features of wireless communications such as erasure rate, packet loss, or packet delivery ratio, introduce new types of uncertainties into networked systems and impact control performance significantly [16]. Impact of communications on networked control systems can be treated by viewing communication systems as added uncertainties and constraints. [19] characterized the impact of noisy communication channels on control performance in a standard feedback loop. [20] treated a communication channel in a control loop as added delays and analyzes dependance of control performance on such delays. [21] modeled communication systems for multi-agent systems as a time-varying network by considering mobility, and established the networked system's control quality. To understand how a communication system can influence a feedback system's performance, [22] established fundamental limitations on control performance when a communication channel is inserted. In [23], an in-depth study of coordinated control and communication design was conducted in which TCP-based communication protocols were employed. [24] concentrated on block erasure channels [25] and established safety distances accordingly.

Platoons communicate via wireless systems. It has been established togeter with experimental verifications that such systems can be reasonably represented by Markov chain mod-

The research of T. Nguyen, L.Y. Wang, and G. Yin was supported in part by the Air Force Office of Scientific Research under FA9550-15-1-0131; the research of H. Zhang was supported in part by the National Science Foundation CAREER award CNS-1054634.

Thu Nguyen is with the Department of Mathematics, Wayne State University, Detroit, MI 48202, nguyenthilethukhtn@gmail.com

Le Yi Wang is with the Department of Electrical and Computer Engineering, Wayne State University, Detroit, Michigan 48202. Email: lywang@wayne.edu

George Yin is with the Department of Mathematics, Wayne State University, Detroit, MI 48202. Email: gyin@math.wayne.edu

Hongwei Zhang is with the Department of Electrical and Computer Engineering, Iowa State University, Ames, IA 50011, Email: hongwei@iastate.edu

Shengbo Li is with the State Key Lab of Automotive Safety and Energy, Tsinghua University, Beijing 100084, China. Email: lisb04@gmail.com

Keqiang Li is with the State Key Lab of Automotive Safety and Energy, Tsinghua University, Beijing 100084, China. Email: likq@tsinghua.edu.cn

els. In particular, Markovian models are shown to be useful representations for binary channels [26], radio communication systems [27], and fading channels [28]. Since mobile wireless communication systems are typical cases of dynamic fading channels, they can be modelled by Markov chains [29]. Employing Markov chains to model communication channels and the weighted-and-constrained consensus (WCC) [30], [31] to coordinate a platoon's operation, this paper provides a modeling and control methodology and impact analysis for highway platoon control under erasure channels. It models the channel interruptions from block erasure and the resulting switching network topologies by Markov chains and derives their probability transition matrices from channels' stochastic characterizations. Impact of communication erasure channels on vehicle platoon formation, robustness, and convergence rate is analyzed and illustrated. As a general framework, the Markov chain model of communication network topologies can also accommodate actively managed networks for resource allocation, interference avoidance, and transmission scheduling.

By comparing convergence properties of networked control algorithms under block erasure channels, we characterize some intrinsic relationships between communication erasure rates and platoon formation convergence performance. The findings of this paper can serve as useful guidelines on communication resource allocations and vehicle coordinations. The main contributions of this paper are the following aspects.

(1) We employ Markov chain models to represent erasure channels and the resulting switching network topologies. Probability transition matrices are derived to represent communication network dynamics.
(2) To study impact of communication erasure channels on platoon control performance, we integrate the Markov chain models of erasure channels with the weighted-and-constrained consensus framework to link communication system features to platoon control.
(3) The relationships among packet delivery ratio, communication resource, network topology structure, and platoon control performance are quantitatively established, and demonstrated by simulation case studies.
(4) We study the impact of communication block erasures on platoon coordination with vehicle dynamic models and illustrate their relationships.

The rest of the paper is arranged as follows. Section II presents networked control algorithms for highway platoon formation and control. Section III introduces Markov chain models for communication erasure channels. Impact of erasure channels on platoon control performance is analyzed in Section IV by establishing convergence rates as functions of the Markov chains for the erasure channels. Section V presents simulation case studies to validate the theoretical conclusions and demonstrate effectiveness of the proposed algorithms. The algorithms are further extended to include vehicle dynamics in Section VI. The impact of erasure channels on such platoon control problems is evaluated. Finally, Section VII presents some potential research problems and points out future directions on integrated control and communications in platoon control.

II. Networked Control Algorithms

We first describe the platoon control framework introduced in [30]. Consider a platoon of $r+1$ vehicles driving in the same lane. The leading vehicle serves as a reference and is labeled as vehicle 0 with position p_n^0 (hence, $p_n^0 = 0$). In the platoon formation, the position of each vehicle is determined by the central point of its length and denoted by $p_n^i, i = 1, \ldots, r$ which is the distance of the ith vehicle to the leading vehicle. The consecutive inter-vehicle distances are denoted by $d_n = [d_n^1, \ldots, d_n^r]'$, where d_n^i is the distance between vehicle i and vehicle $i-1$ at time n and is given by $d_n^i = p_n^i - p_n^{i-1}$for $i = 1, \ldots, r$. The vehicle speeds are $v_n = [v_n^1, \ldots, v_n^r]'$, where z' is the transpose of z. The platoon has a total length L. The goal of platoon control is to distribute the length L appropriately to inter-vehicle distances so that the highway space resource can be optimally utilized and vehicle safety can be enhanced.

Due to disturbances and other factors, at time n, the total actual length of the platoon L_n can be time varying and different from L. On the other hand, in algorithm development, we aim at $L_n = L$ (i.e., maintaining a constant-length platoon). Platoon length variations will be viewed as disturbances to the consensus control problem in this paper. Consequently, in control design, we impose the design constraint

$$\sum_{i=1}^{r} d_n^i = L, \quad n = 0, 1, \ldots \tag{1}$$

Due to terrain conditions and vehicle mass disparity, desired front distances for vehicles differ. For example, a heavy truck needs more front space than a smaller passenger car. Consequently, we introduce a weighting factor γ^i for vehicle i's front distance. It follows that the goal of platoon control is to achieve consensus on the weighted distances d_n^i/γ^i, namely,

$$\frac{d_n^i}{\gamma^i} \to \beta, \ i = 1, \ldots, r,$$

for some constant β. Here, the desired convergence is either with probability one (w.p.1.) or in mean square (MS).

For notational simplicity in the algorithm development, we use $x_n^i = d_n^i$ and denote the states by $x_n = [x_n^1, \ldots, x_n^r]'$, the weighting coefficients by $\gamma = [\gamma^1, \ldots, \gamma^r]'$, and the scaling matrix by $\Psi = \mathrm{diag}[1/\gamma^1, \ldots, 1/\gamma^r]$, respectively. Denote by $\mathbb{1}$ the column vector of all 1s. Together with the constraint (1), the target of the weighted and constrained consensus control is

$$\Psi x_n \to \beta \mathbb{1}$$

subject to $\mathbb{1}' x_n = L$. It follows from $\gamma' \Psi = \mathbb{1}'$ that

$$\beta = \frac{L}{\gamma' \mathbb{1}} = \frac{L}{\gamma^1 + \cdots + \gamma^r}.$$

In our previous work [31], a stochastic approximation algorithm was developed for control of networked systems. At time step n, vehicle platoon control updates x_n to x_{n+1} by the amount u_n

$$x_n^{i+1} = x_n^i + u_n^i, \quad i = 1, \ldots, r \tag{2}$$

where u_n^i is the node control for the i^{th} node, or in a vector form

$$x_{n+1} = x_n + u_n \tag{3}$$

with $x_n = \left[x_n^1, \ldots, x_n^r\right]^{'}, u_n = \left[u_n^1, \ldots, u_n^r\right]^{'}$. These nodes are linked by a network, represented by a directed graph $\mathcal{G}$ whose element (i,j) indicates estimation of the state x_n^j by node i via a communication link and also a permitted control a_n^{ij} (called link control) that adjusts d_n^i and d_n^j coordinately. From its physical meaning, node i can always observe its own state, which is not considered as a link in $\mathcal{G}$. The total number of communication links in $\mathcal{G}$ is l_s.

The idea of the "link control" is motivated by resource sharing: An increase on distance d_i by a_n^{ij} is offset by a decrease on d_j by the same amount so that the total platoon length L remains intact. As a result, the control u_n^i is determined by the link control a_n^{ij} as

$$u_n^i = -\sum_{(i,j)\in\mathcal{G}} a_n^{ij} + \sum_{(j,i)\in\mathcal{G}} a_n^{ji}. \tag{4}$$

The most relevant implication in this control scheme is that for all n,

$$\sum_{i=1}^{r} x_n^i = L, \tag{5}$$

that is, the constraint (1) is always satisfied. Consensus control seeks control algorithms such that $\Psi x_n \to \beta\mathbb{1}$ under the constraint (5).

A link $(i,j) \in \mathcal{G}$ entails an estimate $\widehat{x}_n^{ij}$ of x_n^j by node i with observation noise ξ_n^{ij}. That is

$$\widehat{x}_n^{ij} = x_n^j + \xi_n^{ij}. \tag{6}$$

Let $\tilde{x}_n$ and ξ_n be l_s-dimensional vectors that contain all $\widehat{x}_n^{ij}$ and ξ_n^{ij} in a selected order, respectively. Then, (6) can be written as

$$\tilde{x}_n = H^{\{1\}} x_n + \xi_n, \tag{7}$$

where $H^{\{1\}}$ is an $l_s \times r$ matrix whose rows are elementary vectors such that, if the lth element of $\tilde{x}_n$ is $\widehat{x}_n^{ij}$, then the lth row in $H^{\{1\}}$ is the row vector of all zeros except for a "1" at the jth position. Each link in $\mathcal{G}$ provides information $\delta_n^{ij} = x_n^i/\gamma^i - \widehat{x}_n^{ij}/\gamma^j$, an estimated difference between the weighted x_n^i and x_n^j. This information may be represented by a vector δ_n of size l_s containing all δ_n^{ij} in the same order as $\tilde{x}_n$, where δ_n can be written as

$$\begin{aligned}\delta_n = H^{\{2\}}\Psi x_n - \tilde{\Psi}\tilde{x}_n &= H^{\{2\}}\Psi x_n - \tilde{\Psi}H^{\{1\}}x_n - \tilde{\Psi}_n \\ &= Hx_n - \tilde{\Psi}\xi_n,\end{aligned} \tag{8}$$

where the link scaling matrix $\tilde{\Psi}$ is the $l_s \times l_s$ diagonal matrix whose kth diagonal element is $1/\gamma^j$ if the kth element of $\tilde{x}_n$ is $\widehat{x}_n^{ij}$; $H^{\{2\}}$ is an $l_s \times r$ matrix whose rows are elementary vectors such that, if the lth element of $\tilde{x}(k)$ is $\widehat{x}^{ij}$, then the lth row in $H^{\{2\}}$ is the row vector of all zeros except for a "1" at the ith position, and $H = H^{\{2\}}\Psi - \tilde{\Psi}H^{\{1\}}$.

The information δ_n^{ij} can only be used by nodes i and j. When the platoon control is linear, time invariant, and memoryless, we have $a_n^{ij} = \mu_n g_{ij}\delta_n^{ij}$, where g_{ij} is the link control gain and μ_n is the global time-varying scaling factor which will be used in state updating algorithms as the recursive step-size. Selections of the link gains and μ_n are to ensure convergence of the consensus control. Their further impact on convergence rate will become clearer later. Let G be the $l_s \times l_s$ diagonal matrix that has g_{ij} as its diagonal elements. In this case, the node control becomes $u_n = -\mu_n J^{'} G\delta_n$, where $J = H^{\{2\}} - H^{\{1\}}$. For convergence analysis, we note that μ_n is the global control variable and we may represent u_n equivalently as

$$u_n = -\mu_n J^{'} G(Hx_n - \tilde{\Psi}\xi_n) = \mu_n(Mx_n + W\xi_n), \tag{9}$$

with $M = -J^{'}GH$ and $W = J^{'}G\tilde{\Psi}$. This, together with (3), leads to

$$x_{n+1} = x_n + \mu_n(Mx_n + W\xi_n). \tag{10}$$

It can be directly verified that $\tilde{\Psi}H^{\{1\}}\Psi^{-1} = H^{\{1\}}, H\Psi^{-1} = J, J\mathbb{1} = 0, \Psi^{-1}\mathbb{1} = \gamma$. These imply that $\mathbb{1}^{'}M^{'} = 0, \mathbb{1}^{'}W = 0, M\Psi^{-1}\mathbb{1} = M\gamma = 0$. When the topology changes with time, we use the index θ_n to represent the network topologies. In this case, the system matrices M and W become functions of θ_n, and the stochastic approximation algorithm becomes

$$\begin{aligned}&x_{n+1} = x_n + \mu_n M(\theta_n)x_n + \mu_n W(\theta_n)\xi_n, \\ &\mathbb{1}'x_n = L.\end{aligned} \tag{11}$$

In this paper, the dynamics of the network topology is modeled by a Markov chain: θ_n is a Markov chain taking values in a finite set $A = \{1, \ldots, l_0\}$. The probability transition matrix of θ will be specified in our case studies.

One useful property of $M(\theta)$ is that for each fixed θ, the matrix $M(\theta) \in \mathbb{R}^r \times \mathbb{R}^r$ has the defining property that the transpose $M'(\theta)$ is a generator of a continuous-time Markov chain [31]. Although this matrix does not represent a physical Markov chain, this property is essential in establishing consensus and convergence properties of our algorithms.

To proceed, we use an example to illustrate the steps involved in arriving at the stochastic approximation algorithm (11). This example will also serve as a case for subsequent simulation studies.

Example 2.1: Consider a platoon of five vehicles with total length $L = 82$m. Vehicle i controls the distance d_i, $i = 1, 2, 3, 4$. Then the condition $d_1 + d_2 + d_3 + d_4 = L$ is imposed as a constraint. Suppose that the initial distance distribution among the four vehicles are $d_0^1 = 17.5$m; $d_0^2 = 20.5$m; $d_0^3 = 19$m; $d_0^4 = 25$m. Weighted consensus from vehicle control aims to distribution distance according to the terrain and vehicle conditions defined by $\gamma^1 = 18$, $\gamma^2 = 20$, $\gamma^3 = 24$ and $\gamma^4 = 30$, with the total $\mathbb{1}^{'}\gamma = 92$. As a result,

$$\begin{aligned}&x = (d_1, d_2, d_3, d_4)', \\ &\gamma = (18, 20, 24, 30)', \\ &\Psi = \text{diag}(1/18, 1/20, 1/24, 1/30).\end{aligned}$$

From the total length 82m, the weighted consensus is $d^1 = 16.0435$m; $d^2 = 17.8261$m; $d^3 = 21.3913$m ; $d^4 = 26.7391$m; and the desired weighted average distance is

$$\beta = \frac{L}{\gamma^1 + \gamma^2 + \gamma^3 + \gamma^4} = 0.8913.$$

By choosing the order for the links as $(1,2),(2,1),(3,2),(3,4),(4,3)$ we have

$$\mathcal{G} = \{(1,2),(2,1),(3,2),(3,4),(4,3)\}.$$

It follows that $\widetilde{\Psi} = \text{diag}\begin{bmatrix}1/20 & 1/18 & 1/24 & 1/20 & 1/30 & 1/2\end{bmatrix}$ Suppose that the control gains on the links are selected as $g_{12} = g_{21} = 5, g_{23} = g_{32} = 10$ and $g_{34} = g_{43} = 13$. Then the link control gain matrix is

$$G = \begin{pmatrix} 5 & & & & & \\ & 5 & & & 0 & \\ & & 10 & & & \\ & & & 10 & & \\ & 0 & & & 13 & \\ & & & & & 13 \end{pmatrix} \tag{12}$$

III. Communication Block Erasure Channels

In this paper, we focus on communication erasure channels and their impact on platoon control performance. Under this communication protocol, we will derive Markov chain models for the network topology dynamics in Section IV and present their case studies in Section V.

Block-erasure channels represent channel models where transmitted packets are either received or lost. The loss of a packet may be caused by erasure of one or multiple bits within the packet during transmission. Typically, block-erasure channels are simple models for fading channels. Due to power limitation, transmission noise, signal interference, some codewords in a packet may be completely lost [32], [33], [16]. Probability of packet erasure can be reduced by introducing error detection and correction bits.

For a given communication channel, packet loss is a random process. For simplicity, it is commonly assumed that the process is independent and identically distributed (i.i.d.). However, there are situations in which the present packet-loss probability depends on previous link conditions due to environment conditions or communication system management. Typically environment conditions are temporally related since an underling cause for a link interruption (such as an obstacle in a communication antenna's line of sight) creates a dynamic relationship in consecutive transmissions. This temporal dependence is modeled in this paper by a Markov chain so that a presently connected link can have different packet loss properties from the case when this link is broken.

We consider block-erasure channels with certain channel codings that include error detection. In this protocol, channel error detecting codes such as parity-check matrices are encapsulated and used by the receiver to either detect transmission errors or in some cases correct the missing or erroneous bits. The detection/correction mechanism is shown in Fig. 1. During one round-trip, starting at time t_k, the source generates a data block, which is channel coded with codeword c_{t_k} and transmitted. Due to channel uncertainties, the decoder receives the codeword $\widehat{c}_{t_k}$ with possible erasure of one or more bits. After decoding and error correction, the receiver either acknowledges receipt of the data, or indicates a packet erasure. Under certain pre-designed decision time intervals, transmission of data is confined to the interval $[t_k, t_{k+1})$.

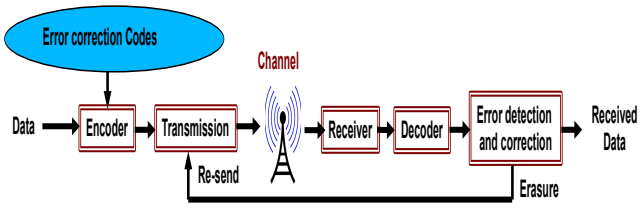

Fig. 1. An erasure channel with error detection and correction and re-transmission

Consequently, re-sending data is permitted only before t_{k+1}. Suppose that the round-trip time for one transmission is τ. If $t_k + \tau < t_{k+1}$, a re-transmission is implemented and the above transmission process renews.

At t_{k+1}, the data are either received correctly or declared to be lost. In the later case, the channel is equivalently disconnected during $[t_k, t_{k+1})$ since no data are received. Since this event is random, the channel is modeled as a random link, with probability p_k to be linked and $1 - p_k$ to be disconnected in this interval. Applying this scenario to all channels, we have a randomly switching network topology such that the probability for each topology is generated from individual link connection probabilities.

Probabilistic models for erasure channels can be derived from channels' signal-to-noise ratio (SNR). In a VANET framework under low density parity-check (LDPC) convolutional coding [34], such models were derived in [23]. When a networked control system is implemented on such block erasure channels with a probabilistic model, for simplicity we assume that all links have a uniform probability ρ to be linked and $1 - \rho$ for erasure, although different link erasure probabilities can also be accommodated. A network of n nodes can have a total of 2^n possible bi-directional links, implying 2^n possible network topologies. This set of topologies forms the state space for the Markov chain θ in (11). If these erasure channels are independent, then the probability distribution of θ can be derived accordingly. We use an example to illustrate this process. The methodology is applicable to both Markovian models and i.i.d. models for erasure channels. In this example, we use i.i.d. channel models, namely, the channels are mutually independent, both spatially and temporally. Examples on the Markovian models will be covered in case studies in Section V.

Example 3.1: Continuing Example 2.1, we now specify the Markov chain $\{\theta_n\}$ in the case of i.i.d. channels. Let $0 \le \rho \le 1$ be the packet delivery ratio. Then $\{\theta_n\}$ is a Markov chain taking values in a finite set $A = \{1, 2, \ldots, 2^{l_s}\} = \{1, 2, \ldots, 64\}$ (since $l_s = 6$ in this example), and $\mathbb{P}(\theta_n = k) = \rho^{l_n^{real}(k)}(1-\rho)^{l_s - l_n^{real}(k)}$, where $l_n^{real}(k) = \sum_{i=1}^{l_s} \lambda_n^i(k)$ is the total number of connected links at time n and $\lambda_n^i(k)$ is an indicator variable showing whether the kth link is up at time n.

The network interconnection is defined by the random

topology matrices

$$H_n^{\{1\}}(k)=\begin{bmatrix}0&\lambda_n^1(k)&0&0\\ \lambda_n^2(k)&0&0&0\\ 0&0&\lambda_n^3(k)&0\\ 0&\lambda_n^4(k)&0&0\\ 0&0&0&\lambda_n^5(k)\\ 0&0&\lambda_n^6(k)&0\end{bmatrix},$$

$$H_n^{\{2\}}(k)=\begin{bmatrix}\lambda_n^1(k)&0&0&0\\ 0&\lambda_n^2(k)&0&0\\ 0&\lambda_n^3(k)&0&0\\ 0&0&\lambda_n^4(k)&0\\ 0&0&\lambda_n^5(k)&0\\ 0&0&0&\lambda_n^6(k)\end{bmatrix},$$

where $\lambda_n^i(k)=\mathbb{1}_{\{y_n^i(k)\le\rho\}},\forall i=1,2,3,4,5,6$ with $y_n^i(k)\sim\mathcal{U}(0,1)$. Consequently, we have

$$\begin{aligned}H_n(k)&=H_n^{\{2\}}(k)\Psi-\widetilde{\Psi}H_n^{\{1\}}(k)\\ J_n(k)&=H_n^{\{2\}}(k)-H_n^{\{1\}}(k)\\ M_n(k)&=-J_n(k)^{'}GH_n(k)\\ W_n(k)&=J_n(k)^{'}G\widetilde{\Psi}.\end{aligned}\tag{13}$$

IV. Convergence and Rate of Convergence

In this section, we employ a Markov chain model for erasure channels and establish convergence and rate of convergence of the algorithm (11). The Markov chain model can be used to represent temporally dependent link properties, link transmission scheduling strategies, co-channel interference avoidance methods, among others.

By embedding erasure channels in our algorithms as a Markov chain, convergence properties become dependent on the erasure channels. Consequently, the main results will allow us to analyze impact of erasure channels on platoon control performance. We begin with the following assumptions.

(A1) The following conditions hold.
- $\mu_n\ge 0$, $\mu_n\to 0$ as $n\to\infty$ and $\sum_n\mu_n=\infty$.
- $\{\theta_n\}$ is a discrete-time Markov chain taking values in A, which is irreducible and aperiodic.
- $\{\xi_n\}$ is a sequence of i.i.d. random variables independent of $\{\theta_n\}$ such that $E|\xi_n|^2<\infty$, $E\xi_n=0$.
- For each $\theta\in A$, $M'(\theta)$ is a generator of a continuous-time Markov chain. [Denote $M'(\theta)=\widetilde{M}(\theta)=(\widetilde{m}_{ij}(\theta))$. Then $\widetilde{m}_{ij}(\theta)\ge 0$ for each $i\ne j$ and $\sum_j\widetilde{m}_{ij}(\theta)=0$ for each i.]
- Denote $\overline{M}=\sum_{k=1}^{l_0}M(k)\nu_k$, where $\nu=(\nu_1,\dots,\nu_{l_0})$ is the stationary distribution associated with the Markov chain $\{\theta_n\}$. Assume that $\overline{M}'=\sum_{k=1}^{l_0}M'(k)\nu_k$ is irreducible.

Remark 4.1: We comment on the assumptions briefly.

- The condition on the step size sequence $\{\mu_n\}$ is not a restriction since it can be selected by the designer. Commonly used sequences include $\mu_n=1/n$, or $\mu_n=1/n^\alpha$ with $0<\alpha<1$, among others.
- Recall that a Markov chain with generator $\overline{M}'$ is said to be irreducible if the system of equations
$$\begin{cases}\nu\overline{M}'=0\\ \nu\mathbb{1}=\sum_{i=1}^{l_0}\nu_i=1\end{cases}$$
has a unique positive solution. The solution $\nu=(\nu_1,\dots,\nu_{l_0})\in\mathbb{R}^{l_0\times l_0}$ is termed a *stationary distribution*.
- As a special case of the assumed Markov chains, the process $\{\theta_n\}$ may be a sequence of i.i.d. random variables taking values in A with $P(\theta_n=k)=p_k$. We assume $p_k>0$ for each $k\in A$.
- If we require an additional condition that for each $k\in A$, $\mathbb{1}'W(k)=0$, then the constraint $\mathbb{1}'x_n=L$ will be automatically satisfied.
- In lieu of the i.i.d. sequence $\{\xi_n\}$, we can treat correlated noises. We use i.i.d. sequences here for simplicity.

Following the ideas of the ODE (ordinary differential equation) method in stochastic approximation [35], define

$$t_n=\sum_{j=0}^{n-1}\mu_j,\ \varpi(t)=\max\{n:t_n\le t\},\tag{14}$$

the piecewise constant interpolation $x^0(t)=x_n$ for $t\in[t_n,t_{n+1})$, and the shift sequence $x^n(t)=x^0(t+t_n)$.

By Gronwall's inequality and a standard argument, we can establish the following assertion: Under (A1), for any $0<T<\infty$,

$$\sup_{n\le\varpi(T)}E|x_n|^2\le K\text{ and }\sup_{0\le t\le T}E|x^n(t)|^2\le K,\tag{15}$$

for some $K>0$, where $\varpi(\cdot)$ is defined in (14). Furthermore, we can obtain the following result.

Theorem 4.2: Under (A1), the iterates x_n generated by algorithm (19) together with the constraint $\mathbb{1}'x_n=L$ satisfy $\Psi x_n\to\beta\mathbb{1}$ or $x_n\to\Psi^{-1}\beta\mathbb{1}=x^*$ w.p.1 as $n\to\infty$.

Outline of proof. We will be very brief since the main technique is from the book of Kushner and Yin [35]. First, it can be shown that $\{x^n(\cdot)\}$ is equi-continuous in the extended sense as defined in [35, p.102]. By the Arzelá-Ascoli theorem (also in the extended sense), we extract any convergent subsequence with limit denoted by $x(\cdot)$. Let $\{\delta_n\}$ be a sequence of real numbers such that $\delta_n\xrightarrow{n}0$, $\sup_{j\ge n}\frac{\mu_j}{\delta_n}\to 0$, and $(\sum_{j=\varpi(n,\ell)}^{\varpi(n,\ell+1)-1}\mu_j)/\delta_n\to 1$ as $n\to\infty$. Then we have for any $t,s>0$,

$$x^n(t+s)-x^n(t)=\sum_{j=\varpi(t_n+t)}^{\varpi(t_n+t+s)-1}\mu_j[M(\theta_j)x_j+W(\theta_j)\xi_j].$$

For each n, choose an increasing sequence $\{\varpi(n,l)\}$ satisfying $n=\varpi(n,1)<\varpi(n,2)<\cdots$ Denote for simplicity $\varpi_l=\varpi(n,l)$. Then

$$\begin{aligned}&x^n(t+s)-x^n(t)\\ &=\sum_{\varpi_l=\varpi(t_n+t)}^{\varpi(t_n+t+s)-1}\delta_n\frac{1}{\delta_n}\sum_{j=\varpi_l}^{\varpi_{l+1}-1}\mu_j[M(\theta_j)x_j+W(\theta_j)\xi_j].\end{aligned}\tag{16}$$

For the first term on the right-hand side of (16), by the continuity of the function $M(\alpha)x$ in x, it is easy to see that the limit of $\frac{1}{\delta_n}\sum_{j=\varpi_l}^{\varpi_{l+1}-1}\mu_j M(\theta_j)x_j$ is the same as that of

$$\begin{aligned}&\frac{1}{\delta_n}\sum_{j=\varpi_l}^{\varpi_{l+1}-1}\mu_j M(\theta_j)x_{\varpi_l}\\&=\frac{1}{\delta_n}\sum_{j=\varpi_l}^{\varpi_{l+1}-1}\mu_j[M(\theta_j)-\overline{M}]x_{\varpi_l}+\frac{1}{\delta_n}\sum_{j=\varpi_l}^{\varpi_{l+1}-1}\mu_j\overline{M}x_{\varpi_l}.\end{aligned}\tag{17}$$

Since $\{\theta_n\}$ is a finite state Markov chain that is irreducible and aperiodic, it is well known (see [36, p. 488]) that $\{\theta_n\}$ is ergodic. That is, $(1/n)\sum_{j=1}^{n}M(\theta_j)$ converges to its mean with respect to the stationary distribution $\{\nu_j : j\le m\}$. Thus the first term in the last line of (17) converges to 0 w.p.1, whereas as $n\to\infty$,

$$\sum_{\varpi_l=\varpi(t_n+t)}^{\varpi(t_n+t+s)-1}\delta_n\frac{1}{\delta_n}\sum_{j=\varpi_l}^{\varpi_{l+1}-1}\mu_j\overline{M}x_{\varpi_l}\to\int_t^{t+1}\overline{M}x(u)du.$$

Likewise, we can show that $\sum_{j=\varpi(t_n+t)}^{\varpi(t_n+t+s)-1}\mu_j W(\theta_j)\xi_j\to 0$ w.p.1 as $n\to\infty$. Combining the above arguments together, we obtain that the limit satisfies the ODE

$$\dot{x}=\overline{M}x.\tag{18}$$

The irreducibility of $\overline{M}'$ implies that the stationary point of (18) is given by $x^*=\Psi^{-1}\beta\mathbb{1}$ in view of the constraint. Using the methods of [37], we can then conclude the proof. □

Using Remark 4.1, the above argument is based on the assumption that $\{\theta_n\}$ is a Markov chain. If we are dealing with an i.i.d. sequence $\{\theta_n\}$, then ν_k above is replaced by p_k. The proof in fact will be simpler.

To improve convergence rate, we use the idea of post-iterate averaging in [35, Chapter 11], resulting in a two-stage stochastic approximation algorithm. We first obtain a coarse approximation by using a sequence of relatively large step sizes, and then we refine it by taking an iterate average. For simplicity, we select $\mu_n=1/n^\gamma$ for some $(1/2)<\gamma<1$. The algorithm is given as follows:

$$\begin{aligned}x_{n+1}&=x_n+\frac{1}{n^\gamma}M(\theta_n)x_n+\frac{1}{n^\gamma}W(\theta_n)\xi_n,\\\overline{x}_{n+1}&=\overline{x}_n-\frac{1}{n+1}\overline{x}_n+\frac{1}{n+1}x_{n+1}.\end{aligned}\tag{19}$$

We further assume $\mathbb{1}'W(k)=0$ for each $k\in A$. Then $\mathbb{1}'\overline{x}_n=L$.

To emphasize the dimension of the vector $\mathbb{1}$, we sometimes write $\mathbb{1}_\kappa$ for an integer κ in what follows. Since $\overline{M}$ is assumed to have rank $r-1$, without loss of generality, assume that the first $r-1$ columns are independent. For each $k\in A$, partition the matrices $M(k)$ and $W(k)$ as

$$M(k)=\begin{pmatrix}M_{11}(k)&M_{12}(k)\\M_{21}(k)&M_{22}(k)\end{pmatrix},\tag{20}$$

$$W(k)=\begin{pmatrix}W_{11}(k)&W_{12}(k)\\W_{21}(k)&W_{22}(k)\end{pmatrix}$$

where $M_{11}(k)\in\mathbb{R}^{(r-1)\times(r-1)}$, $M_{12}(k)\in\mathbb{R}^{(r-1)\times 1}$, $M_{21}(k)\in\mathbb{R}^{(r-1)\times 1}$, $M_{22}(k)\in\mathbb{R}^{1\times 1}$, and similarly for $W_{ij}(k)$. Accordingly, we partition x_n, $\overline{x}_n$, and $W(k)$ as

$$x_n=\begin{pmatrix}\widetilde{x}_n\\x_{n,r}\end{pmatrix},\ \overline{x}_n=\begin{pmatrix}\Xi_n\\\overline{x}_{n,r}\end{pmatrix},\ \xi_n=\begin{pmatrix}\widetilde{\xi}_n\\\xi_{n,r}\end{pmatrix},\tag{21}$$

respectively, with compatible dimensions as those of $M(k)$ for each $k\in A$.

It follows from (19) that

$$\begin{cases}\widetilde{x}_{n+1}&=\widetilde{x}_n+\frac{1}{n^\gamma}\widetilde{M}(\theta_n)\widetilde{x}_n\\&\quad+\frac{1}{n^\gamma}[W_{11}(\theta_n)\widetilde{\xi}_n+W_{12}(\theta_n)\xi_{n,r}]\\&\quad+\frac{1}{n^\gamma}M_{12}(\theta_n)(L-\mathbb{1}'_{r-1}\widetilde{x}_n)\\\Xi_{n+1}&=\Xi_n-\frac{1}{n+1}\Xi_n+\frac{1}{n+1}\widetilde{x}_{n+1},\end{cases}\tag{22}$$

where $\widetilde{M}(k)=M_{11}(k)-M_{12}(k)\mathbb{1}'_{r-1}$. Note that $x_{n,r}=L-\mathbb{1}'_{r-1}\widetilde{x}_n$ and $\overline{x}_{n,r}=L-\mathbb{1}'_{r-1}\Xi_n$.

Define

$$\overline{M}_0=\sum_{k=1}^{l_0}\nu_k\widetilde{M}(k),\ \overline{M}_{12}=\sum_{k=1}^{l_0}\nu_k M_{12}(k),$$
$$\overline{W}_{11}=\sum_{k=1}^{l_0}\nu_k W_{11}(k),\ \text{ and }\ \overline{W}_{12}=\sum_{k=1}^{l_0}\nu_k W_{12}(k).$$

We assume that $\overline{M}_0$ is nonsingular. Denote $x^*=(\check{x}^*,x_r^*)'$, where $\check{x}^*$ is the first $(r-1)$-dimensional vector of x^* and x_r^* is the last component. Similar to Theorem 4.2, denote the interpolated and shifted sequence by $\widetilde{x}^n(t)$. It then can be shown that any convergent subsequence of $\widetilde{x}^n(\cdot)$ has the limit

$$\frac{d}{dt}\widetilde{x}(t)=\overline{M}_0\widetilde{x}(t)+\overline{M}_{12}L.$$

The stationary point of the above ODE is $-(\overline{M}_0)^{-1}\overline{M}_{12}L$.

$$\widetilde{x}_n\to\widetilde{x}^*=-(\overline{M}_0)^{-1}\overline{M}_{12}L\ \text{ and }\ \Xi_n\to\widetilde{x}^*\ \text{ as }\ n\to\infty.$$

Next, define

$$\widetilde{B}_n(t)=\frac{1}{\sqrt{n}}\sum_{j=0}^{\lfloor nt\rfloor-1}[\overline{W}_{11}\widetilde{\xi}_j+\overline{W}_{12}\xi_{j,r}].\tag{23}$$

Define also

$$\overline{B}_n(t)=\sqrt{n}[\overline{x}_{\lfloor nt\rfloor+1}-\widetilde{x}^*]\ \text{ for }\ t\in[0,1],\tag{24}$$

where $\lfloor z\rfloor$ denotes the integer part of z. Then it can be shown that $\overline{B}_n(t)=-\overline{M}_0^{-1}\widetilde{B}_n(t)+o(1)$, where $o(1)\to 0$ in probability. The details of the argument can be found on [38], [39], which is omitted here.

Theorem 4.3: Under (A1) and assuming that $\widetilde{\xi}_n$ and $\xi_{n,r}$ are independent, the following assertions hold:

- $\overline{B}_n(\cdot)$ converges weakly to $\overline{B}(\cdot)$, a Brownian motion with covariance $\overline{M}_0^{-1}\Sigma_0(\overline{M}_0^{-1})'t$, where $\Sigma_0=\overline{W}_{11}E(\widetilde{\xi}_1\widetilde{\xi}_1')\overline{W}_{11}'+\overline{W}_{12}E(\xi_{1,r}\xi_{1,r}')\overline{W}_{12}'$;
- $\sqrt{n}(\widetilde{x}_n-\widetilde{x}_*)$ converges in distribution to a normal random variable with mean 0 and asymptotic covariance $\overline{M}_0^{-1}\Sigma_0(\overline{M}_0^{-1})'$.

We point out that the asymptotic covariance is a main performance indicator for the convergence rate. As a result, to study impact of erasure channels on convergence rates, we primarily use this covariance matrix to evaluate how fast convergence to platoon formation can be achieved and how this rate depends on the channel erasure ratio (or equivalently, the packet delivery ratio). Such studies will be carried out by case studies in the next section.

V. Simulation Case Studies

In this section, the performance of the Weighted and Constrained Consensus Control Algorithm (WCCCA) (11) in the block eraser channel problem is assessed through two different models. The system under study is defined as in Example 2.1. In addition, we include observation noises, represented by an i.i.d. sequence $\{\xi_n\}$ of Gaussian noises with mean 0 and variance 1. In all the numerical results, we have run 100 times the WCCCA that utilizes a sequence of stepsizes $\mu_n = \frac{0.1}{n^{0.04}}$.

Example 5.1: We first consider the i.i.d. erasure channels specified in Example 3.1. To illustrate the impact of packet delivery ratio on convergence rate of the WCCCA, four different values of the packet delivery ratio ρ are compared: $0.4, 0.8, 0.9$ and 1. In order to obtain these results, we have run the WCCCA 100 times. The results are summarized in Tables I and II. Table I shows the mean square errors (MSE) of weighted consensus with respect to different packet delivery ratios and numbers of iteration steps. Apparently, the higher the packet delivery ratio is, the smaller the consensus error becomes. Also, the longer the iteration steps are, the smaller the consensus errors become.

In Table II, we compare the sample variances of $\Xi_n - \tilde{x}^*$

$$\bar{S}_n = (1/n)\sum_{j=1}^{n}(\Xi_j - \tilde{x}^*)'(\Xi_j - \tilde{x}^*)$$

by the WCCCA algorithm to these of $\tilde{x}_n - \tilde{x}^*$

$$S_n = (1/n)\sum_{j=1}^{n}(\tilde{x}_j - \tilde{x}^*)'(\tilde{x}_j - \tilde{x}^*)$$

by adding the post-iterate averaging algorithm. The results demonstrate that the post-iterate averaging algorithm performs better, with smaller $\bar{S}_n$, than the original one for large n. In addition, $\bar{S}_n$ is larger when the packet delivery ratio is reduced. Furthermore, it appears that the post-iterate averaging procedure demonstrates more accuracy and more robust convergence rates.

TABLE I
Mean square errors between the desired consensus states and the estimated ones.

Iteration	ρ	MSE of the estimator for			
		d_1	d_2	d_3	d_4
$N = 300$	$\rho = 1$	0.1719	0.0986	0.0779	0.2068
	$\rho = 0.9$	0.1910	0.1093	0.0867	0.2281
	$\rho = 0.8$	0.2217	0.1320	0.1021	0.2648
	$\rho = 0.7$	0.2605	0.1458	0.1140	0.3071
$N = 500$	$\rho = 1$	0.1052	0.0638	0.0529	0.1270
	$\rho = 0.9$	0.1168	0.0707	0.0583	0.1405
	$\rho = 0.8$	0.1333	0.0781	0.0635	0.1603
	$\rho = 0.7$	0.1615	0.1044	0.0811	0.1962

TABLE II
Comparison between S_n from the traditional algorithm and $\bar{S}_n$ from the post-iterate averaging algorithm.

Iteration	S_n	$\overline{S}_n$			
	$\rho = 1$	$\rho = 1$	$\rho = 0.9$	$\rho = 0.8$	$\rho = 0.7$
100	4.6131	3.1069	3.5049	4.0216	4.3711
200	4.2182	1.8284	2.1008	2.4456	2.6853
300	4.0053	1.3276	1.5367	1.7791	1.9850
400	3.8980	1.0514	1.2221	1.4116	1.5876
500	3.8521	0.8756	1.0196	1.1758	1.3291
600	3.7931	0.7550	0.8796	1.0114	1.1473
700	3.7562	0.6647	0.7748	0.8879	1.0110
800	3.7210	0.5946	0.6932	0.7929	0.9059
900	3.7083	0.5391	0.6286	0.7182	0.8224
1000	3.6799	0.4940	0.5758	0.6575	0.7545

We now demonstrate the effectiveness of the WCCCA and the impact of block erasure channels on platoon formation. Fig. 2 shows inter-vehicle distance trajectories. It is clear that the WCCCA achieves fast convergence: with only a relatively small number of iterations, the inter-vehicle distances have distributed close to the desired weighted consensus. By comparing convergence rates under different packet delivery ratios in the four subplots, we can see that convergence is faster if the packet delivery ratio is higher. From these results, it is also clear that the WCCCA is robust against erasure channel uncertainties, evidenced by convergence under all levels of packet delivery ratios.

We finally assess asymptotic efficiency of the algorithm by comparing sample variances with respect to the Cramér-Rao lower bounds under different packet delivery ratios. Fig. 3 shows that the scaled empirical variances approach the theoretical Cramér-Rao lower bounds. The convergence speeds obtained based on the four choices of ρ are further compared in Table III, which indicates that the packet delivery ratio ρ impacts convergence rates significantly. Since the WCCCA achieves asymptotically the Cramér-Rao lower bounds, the relationship between the packet delivery ratio and convergence rate in Table III is fundamental, in the sense that to further improve convergence rate, communication resources must be assigned to increase the packet delivery ratio.

TABLE III
Covariances of weighted consensus errors obtained from simulation based on 4 different choices of ρ.

Iteration	Covariance			
	$\rho = 1$	$\rho = 0.9$	$\rho = 0.8$	$\rho = 0.7$
500	0.0837	0.0853	0.0887	0.0907
1000	0.0856	0.1069	0.1117	0.1126
1500	0.0431	0.0478	0.0505	0.0512
2000	0.0244	0.0269	0.0284	0.0289
2500	0.0154	0.0172	0.0181	0.0184
3000	0.0107	0.0120	0.0128	0.0130

Example 5.2: This example evaluates the performance of WCCCA in the block erasure channel problem for a larger platoon. Consider a platoon of eleven vehicles with total length $L = 220$. Assume that $d_0^1 = 17.5$m; $d_0^2 = 20.5$m; $d_0^3 = 19$; $d_0^4 = 25$m; $d_0^5 = 22$m; $d_0^6 = 30$m; $d_0^7 = 18.5$m; $d_0^8 = 27$m; $d_0^9 = 16.5$m; $d_0^{10} = 24$m and $\gamma^1 = 18$, $\gamma^2 = 20$; $\gamma^3 = 24$; $\gamma^4 = 30$; $\gamma^5 = 22$; $\gamma^6 = 28$; $\gamma^7 = 36$; $\gamma^8 = 32$; $\gamma^9 = 40$;

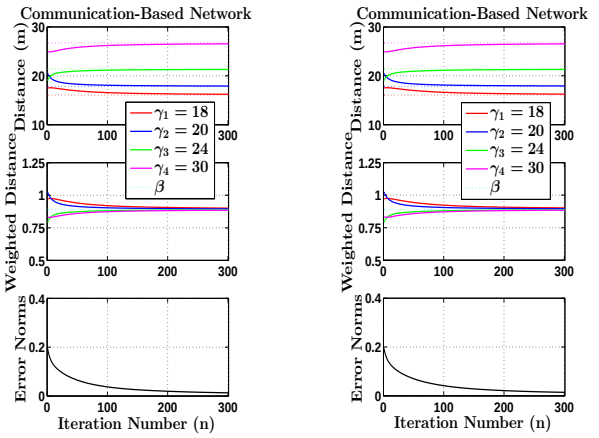

(a) $\rho = 1$ (b) $\rho = 0.9$

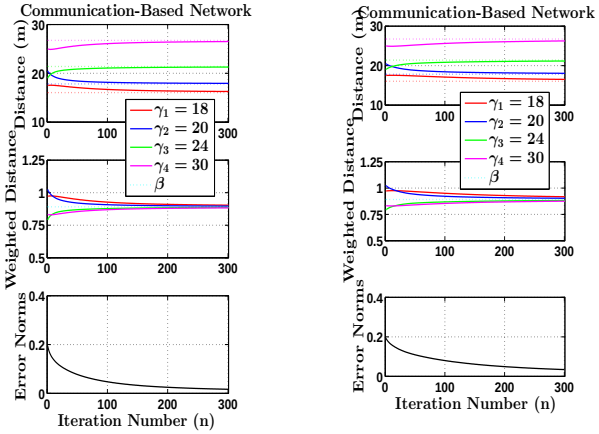

(c) $\rho = 0.8$ (d) $\rho = 0.4$

Fig. 2. Platoon control performance under communication erasure channels.

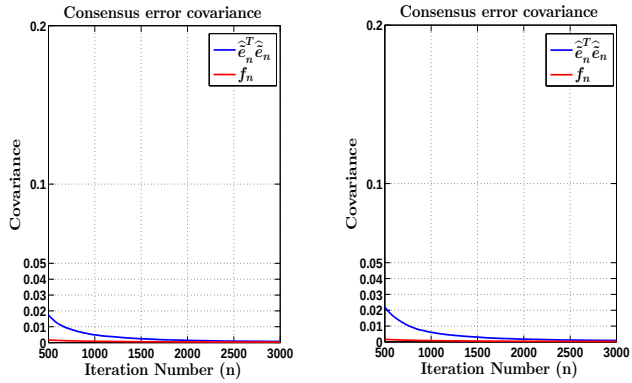

(a) $\rho = 1$ (b) $\rho = 0.9$

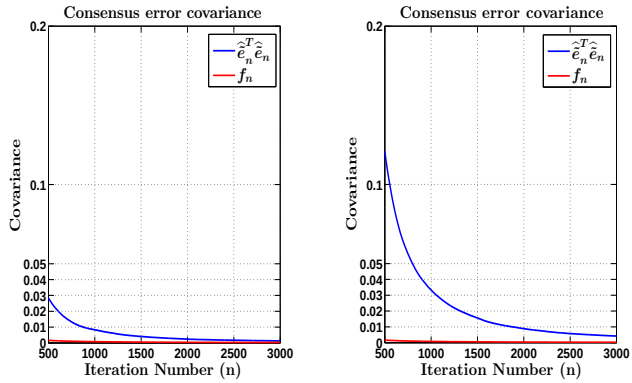

(c) $\rho = 0.8$ (d) $\rho = 0.4$

Fig. 3. Evolution of the theoretical asymptotic covariance $f_n = \frac{Trace\left(\overline{M}_0^{-1}\Sigma_0(\overline{M}_0^{-1})'\right)}{n}$ and the empirical one obtained by simulation $\widehat{\widehat{e}}_n^T\widehat{\widehat{e}}_n$.

$\gamma^{10} = 34$. Suppose that

$$\mathcal{G} = \{(1,2),(2,1),(2,3),(3,2),(3,4),(4,3),(4,5),(5,4),(5,6),(6,6),(6,7),(7,6),(7,8),(8,7),(8,9),(9,8),(9,10),(10,9)\}.$$

and $g_{12} = g_{21} = 5$, $g_{23} = g_{32} = 10$,$g_{34} = g_{43} = 13$, $g_{45} = g_{54} = 15$, $g_{56} = g_{65} = 17$, $g_{67} = g_{76} = 19$,$g_{78} = g_{87} = 21$, $g_{89} = g_{98} = 25$ and $g_{910} = g_{109} = 30$.

The effectiveness of the WCCCA on the platoon control in the block erasure channels problem is illustrated by all related quantities plotted in Fig. 4 and Fig. 5. They show that the algorithm performs for a larger platoon. However, it takes longer time to converge to consensus than in the case of Example 5.1.

Example 5.3: In this example, the impact of communication erasure channels and the effectiveness of the WCCCA on platoon control performance are further studied by expanding the erasure channel model in Example 5.1 to a Markov chain mode. The same system as in Example 5.1 is considered. For illustration, we randomly generate a transition matrix P of dimension $l_0 \times l_0$ of the Markov chain $\{\theta_n\}$. Due to the size of the matrix we report below some parts of it only. The full matrix is available upon request.

$$P = \begin{bmatrix} 0.0049 & 0.0160 & 0.0283 & \dots & 0.0015 & 0.0230 & 0.0305 \\ 0.0079 & 0.0308 & 0.0021 & \dots & 0.0186 & 0.0225 & 0.0006 \\ 0.0033 & 0.0203 & 0.0083 & \dots & 0.0138 & 0.0309 & 0.0097 \\ \vdots & \vdots & \vdots & \ddots & \vdots & \vdots & \vdots \\ 0.0294 & 0.0285 & 0.0072 & \dots & 0.0091 & 0.0169 & 0.0266 \\ 0.0060 & 0.0132 & 0.0047 & \dots & 0.0144 & 0.0257 & 0.0221 \\ 0.0338 & 0.0099 & 0.0209 & \dots & 0.0090 & 0.0159 & 0.0150 \end{bmatrix}$$

In such a case, $\mathbb{P}(\theta_n = k) = \pi_k$, where $\pi = (\pi_1, \dots, \pi_{64})$ is the stationary distribution of the Markov chain satisfying the condition $\pi P = \pi$. Fig. 6 presents the inter-vehicle distance trajectories as well as the sample variance with respect to the Cramér-Rao lower bounds. As in the previous example, it is also interesting to see that the WCCCA has the potential to attenuate the block erasure channel's impact on the platoon formation and is robust against erasure channel uncertainties under the Markov chain model. These simulation results further demonstrate the impact of communication erasure channels on vehicle platoon formation and the robustness

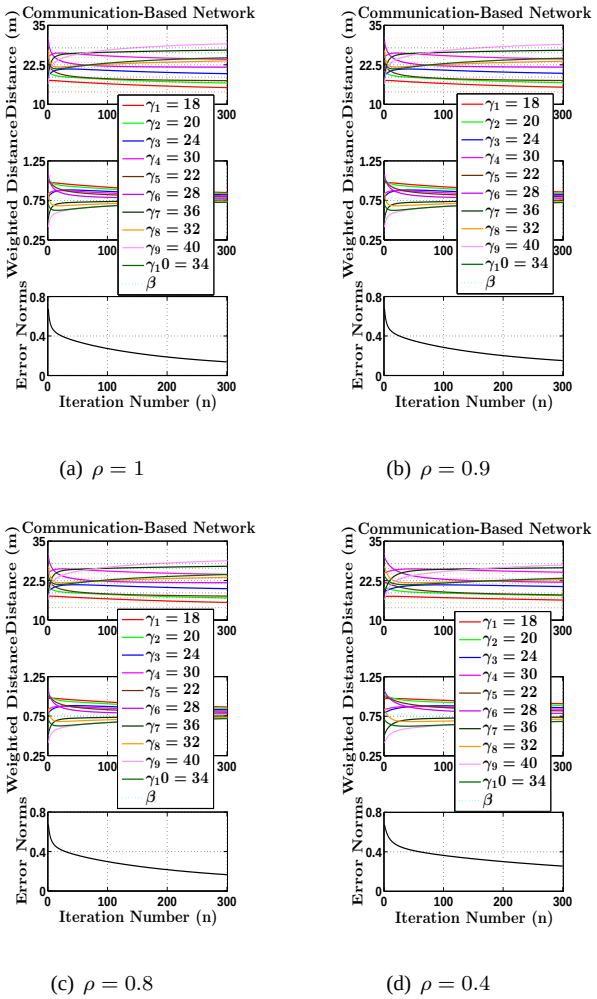

(a) $\rho = 1$ (b) $\rho = 0.9$

(c) $\rho = 0.8$ (d) $\rho = 0.4$

Fig. 4. Platoon control performance under communication erasure channels for larger platoon.

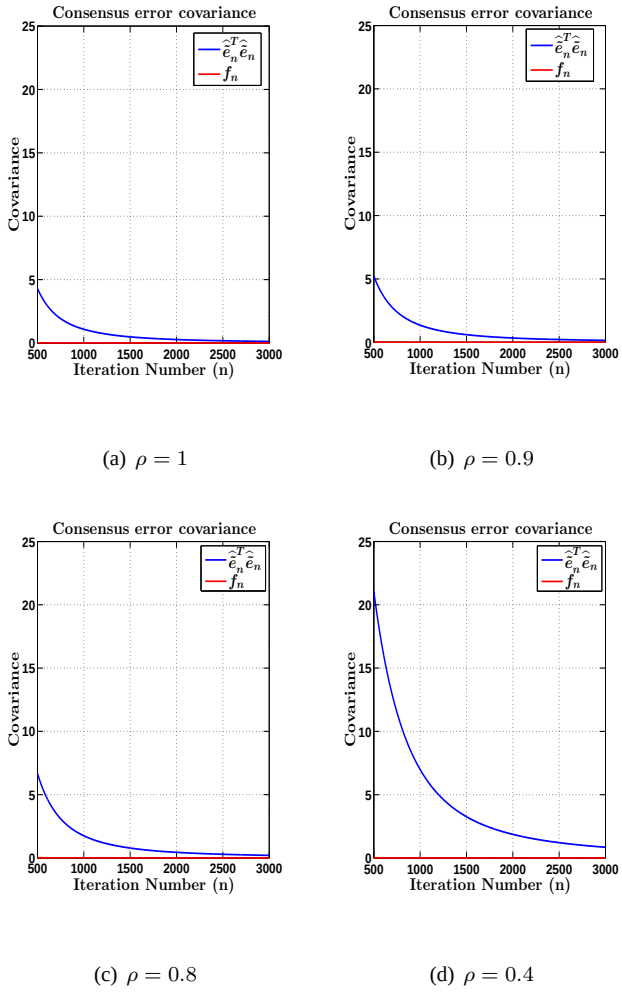

(a) $\rho = 1$ (b) $\rho = 0.9$

(c) $\rho = 0.8$ (d) $\rho = 0.4$

Fig. 5. Evolution of the theoretical asymptotic covariance $f_n = \frac{Trace\left(\overline{M}_0^{-1}\Sigma_0(\overline{M}_0^{-1})'\right)}{n}$ and the empirical one obtained by simulation $\widehat{\widetilde{e}}_n^T\widehat{\widetilde{e}}_n$ for larger platoon.

under the WCCCA.

Example 5.4: In this example, we demonstrate the performance of the algorithm when the erasure channel is a Markov chain. For comparison with Example 5.1, we create a Markov chain $\{\theta_n\}$ whose invariant distribution is the same as the case in Example 5.1.

All related quantities are plotted in Fig. 7 and Fig. 8. The simulation results show that our algorithm still performs well in this case. However, due to the dependent structure of the transition matrix, it takes longer time for convergence to consensus than the one in Example 5.1.

VI. Interaction with Vehicle Dynamics

In Sections III-V, we have focused on the impact of communication block erasures on platoon coordination, under an ideal assumption that control demands are implemented without any delay or dynamics. In practical systems, when a demand wants to change a vehicle's speed or position, the control action is an applied torque on the vehicle. The vehicle's response to such a control input is subject to the vehicle dynamics. Interconnection and interaction between information gathering and

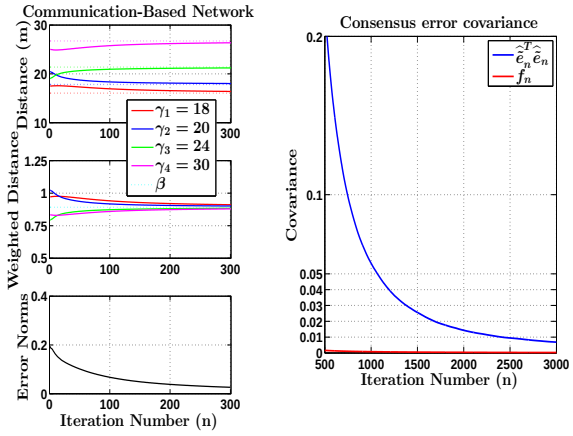

(a) Platoon control performance (b) Sample Variance

Fig. 6. Platoon control performance under Markovian communication erasure channels.

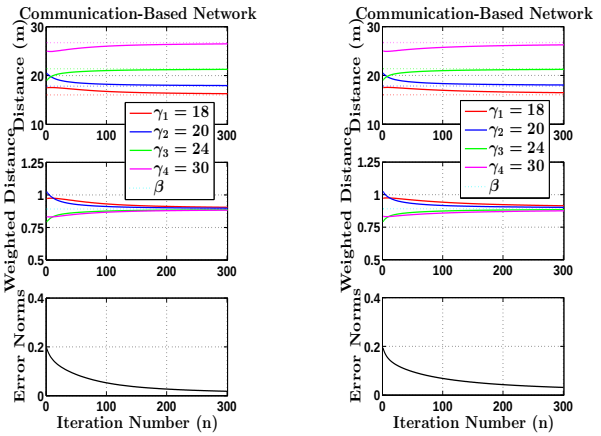

(a) $\rho = 1$ (b) $\rho = 0.9$

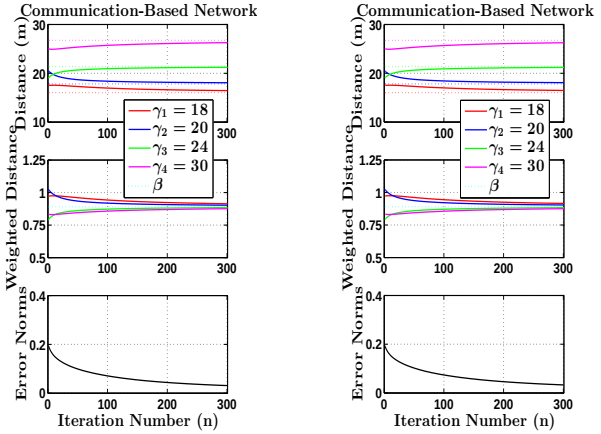

(c) $\rho = 0.8$ (d) $\rho = 0.7$

Fig. 7. Platoon control performance under Markovian communication erasure channels.

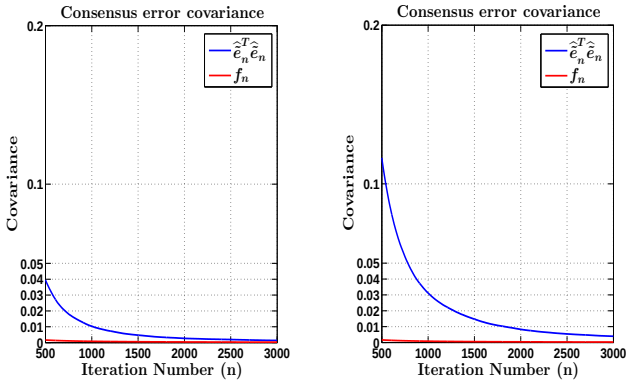

(a) $\rho = 1$ (b) $\rho = 0.9$

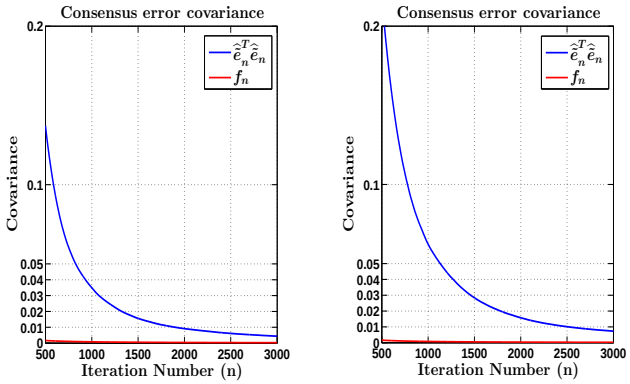

(c) $\rho = 0.8$ (d) $\rho = 0.7$

Fig. 8. Evolution of the theoretical asymptotic covariance $f_n = \frac{Trace\left(\overline{M}_0^{-1}\Sigma_0(\overline{M}_0^{-1})'\right)}{n}$ and the empirical one obtained by simulation $\hat{\tilde{e}}_n^T\hat{\tilde{e}}_n$ under Markovian communication erasure channels.

decision making at the higher level (cyber space) and vehicle control (physical space) were discussed in [30].

In this section, we include vehicle dynamics and evaluate impact of communication block erasures on platoon coordination under a more realistic environment. Inclusion of vehicle dynamics creates a two-layer structure. When the consensus control generates an action toward a desired platoon formation, it serves as a command to the local controller for execution. Due to vehicle dynamics and road/traffic conditions, execution of such control actions encounters standard performance limitations such as steady-state errors, overshoot, rising time, delay, and other relevant performance measures. For detailed studies on platoon stability under both communication links and vehicle dynamics, we refer the reader to [30]. This section concentrates on erasure channels.

A. Vehicle Dynamics and Normalization

The dynamics of the jth vehicle follows the basic law

$$m_j \dot{v}_j = F_j - L_j^0(\dot{v}_j) + \varepsilon_j^0 \tag{25}$$

where m_j is the mass of the vehicle, F_j is the vehicle driving force (when it is positive) or braking force (when it is negative), $L_j^0(\dot{v}_j)$ is the modeled load force (which is known and can be used in control action), and ε_j^0 is the uncertainty term which captures modeling errors, unknown factors on tires, roads, weather conditions, measurement noise, etc. Normalization of (25) results in

$$\begin{aligned}\dot{v}_j &= \frac{F_j}{m_j} - \frac{L_j^0(\dot{v}_j)}{m_j} + \frac{\varepsilon_j^0}{m_j} \\ &= u_j - L_j(\dot{v}_j) + \varepsilon_j = w_j + \varepsilon_j.\end{aligned}$$

Here, $u_j = F_j/m_j$ is the control variable, $L_j(\dot{v}_j) = L_j^0(\dot{v}_j)/m_j$ is the normalized drag, $\varepsilon_j = \varepsilon_j^0/m_j$ is the normalized uncertainty, and $w_j = u_j - L_j(\dot{v}_j)$ is a linearized control input.

Together with $p_j(t)$, the position of j^{th} vehicle at time t, we have

$$\begin{cases} \dot{p}_j &= v_j, \\ \dot{v}_j &= w_j + \varepsilon_j, \\ y_j &= p_j,\ j = 1, \ldots, r. \end{cases} \tag{26}$$

Define $\eta_j = [p_j, v_j]'$. We have

$$\dot{\eta}_j = A\eta_j + Bw_j + B\varepsilon_j; \quad y_j = C\eta_j \tag{27}$$

with $A = \begin{bmatrix} 0 & 1 \\ 0 & 0 \end{bmatrix}$, $B = \begin{bmatrix} 0 \\ 1 \end{bmatrix}$, $C = [1, 0]$, noting that the matrices A, B, and C are same for all j due to normalization and input linearization.

B. Platoon Dynamics and Vehicle Control

The consensus control strategies based on algorithm (11) produce the desired distances $d(t) = [d_1(t), \ldots, d_r(t)]'$ in the presence of block communication erasure channels at the decision time t . For the jth vehicle, $d_j(t_k)$, the distance of the jth vehicle to its front vehicle (the $(j-1)$th vehicle), will be the command to the vehicle's on-board dynamic controller. The actual vehicle distance will be denoted by $\widetilde{d}_j(t)$. The local control is then a tracking control that follows $d_j(t_k)$ during $t \in [t_k, t_{k+1})$. Due to dynamics of the vehicle control systems, the actual inter-vehicle distance trajectories $\widetilde{d}(t_k) = [\widetilde{d}_1(t_k), \ldots, \widetilde{d}_r(t_k)]'$ are different from $d(t) = [d_1(t), \ldots, d_r(t)]'$. As a result, they create a cyber-physical interaction which influences substantially the platoon control performance.

We first build the entire platoon dynamics from the linearized and normalized vehicle dynamics (27)

$$\dot{\eta}_j = A\eta_j + Bw_j + B\varepsilon_j; \quad y_j = C\eta_j, j = 1, \ldots, r.$$

Denote $y = [y_1, \ldots, y_r]'$, $w = [w_1, \ldots, w_r]'$, $\eta = [\eta_1', \ldots, \eta_r']'$, $\varepsilon = [\varepsilon_1, \ldots, \varepsilon_r]'$. Let I_r be the r-dimensional identity matrix. Define the block diagonal matrices $\widetilde{A} = I_r \otimes A$, $\widetilde{B} = I_r \otimes B$, $\widetilde{C} = I_r \otimes C$, where $\otimes$ is the Kronecker product [40]. Then the platoon dynamics is

$$\dot{\eta} = \widetilde{A}\eta + \widetilde{B}w + \widetilde{B}\varepsilon; \quad y = \widetilde{C}\eta.$$

For the jth vehicle, the controller F_j will be designed based on the A, B, C, and the tracking error $e_j(t) = d_j(t) - \widetilde{d}_j(t)$ in the following feedback structure [41]

$$\dot{z}_j = e_j; w_j = -K\eta_j + k_0 z_j, \tag{28}$$

which includes both the state feedback term $-K\eta_j$ for stability and transient performance, and the integral output feedback $k_0 z_j$ for eliminating steady-state tracking errors. Since the linearized and normalized subsystems have the same A, B, and C matrices, the controller matrices k_0 and K will also be uniform over all subsystems.

By denoting $z = [z_1', \ldots, z_r']'$, $e = [e_1, \ldots, e_r]'$, $\widetilde{K} = I_r \otimes K$, the controller for the platoon is

$$\dot{z} = e; w = -\widetilde{K}\eta + k_0 z.$$

Note that $\widetilde{d}_1 = p_1 - p_0$, ..., $\widetilde{d}_r = p_r - p_{r-1}$, where the leading vehicle's position p_0 is external to the system as the time-varying reference to the platoon. Then, $e_1 = d_1 - (p_1 - p_0)$, ..., $e_r = d_r - (p_r - p_{r-1})$. The platoon dynamics is represented by

$$\begin{cases} \dot{z} &= e \\ \dot{\eta} &= \widetilde{A}\eta + \widetilde{B}w + \widetilde{B}\varepsilon \\ w &= -\widetilde{K}\eta + k_0 z \\ e &= -S\widetilde{C}\eta + B_1 p_0 + d \end{cases} \tag{29}$$

where

$$S = \begin{bmatrix} 1 & 0 & \cdots & 0 & 0 \\ -1 & 1 & \cdots & 0 & 0 \\ \vdots & & & & \vdots \\ 0 & 0 & \cdots & -1 & 1 \end{bmatrix}; B_1 = \begin{bmatrix} 1 \\ 0 \\ \vdots \\ 0 \end{bmatrix}.$$

C. Examples

For illustration, we use the system in Example 5.1 to demonstrate integration of platoon consensus decision and vehicle control. Since Example 5.1 does not involve vehicle dynamics, the convergence rate is expressed in terms of the number of iteration steps. When the vehicle dynamics is introduced, the vehicle signal processing sampling time is introduced. The sampling rate is usually quite high. As a result, the actual convergence speed of platoon consensus control is predominantly determined by how fast the vehicles can be controlled to follow the decisions from the cyber space. In the following case studies, the sampling rate is 100 Hz, and consensus control is shown with respect to the clock time.

Example 6.1: Consider the system in Example 5.1 with the same initial distance distribution among the five vehicles are $d_1^0 = 17.5$ m; $d_2^0 = 20.5$ m; $d_3^0 = 19$ m; $d_4^0 = 25$ m; and the same weighting $\gamma^1 = 18$, $\gamma^2 = 20$, $\gamma^3 = 24$ and $\gamma^4 = 30$, with the total weight $\mathbb{1}'\gamma = 92$. At each decision point, the consensus control of Example 3.1 issues a new distance distribution d_k^1, d_k^2, d_k^3, d_k^4. These desired distances will be communicated to the vehicles as the commend signals. The vehicles' on-board controllers will implement their tracking control according to

$$\dot{z}_j = e_j = k_0(d_j - (C\eta_j - p_{j-1})); w_j = -[k_1, k_2]\eta_j + k_0 z_j, \tag{30}$$

where p_{j-1} is an external signal to the jth vehicle. The control parameters are selected as $k_0 = 4.096$, $k_1 = 7.68$, $k_2 = 4.8$, which will place the poles of the local closed-loop systems at $-1, -1, -1$.

Suppose that the link observation noises are i.i.d. sequences of Gaussian random variables with mean zero and variance 1. Fig. 9 shows the inter-vehicle distance trajectories. Starting from a platoon formation, suppose that a sudden braking of the leading vehicle results in a sudden distance change in d_1 by 4 m. This disturbance causes initially a large deviation of the platoon formation. The top plot shows how distances are gradually distributed according to the desired distributions. The middle plot illustrates that the weighted distances converge to a constant. The weighted consensus error trajectories are plotted in the bottom plot.

Example 6.2: The impact of vehicle control can be further studied. Suppose that for the system in Example 6.1, a more aggressive control action is adopted. The vehicle controller is designed to place the poles of the local closed-loop systems at $-1.4, -1.4, -1.4$. The corresponding control parameters are $k_0 = 8$, $k_1 = 12$, $k_2 = 6$. Since the larger control gains are used, more engine torques will be used in vehicle control. Suppose that the link observation noises are i.i.d. sequences of Gaussian random variables with mean zero and variance 1. Fig. 10 shows the inter-vehicle distance trajectories. Starting

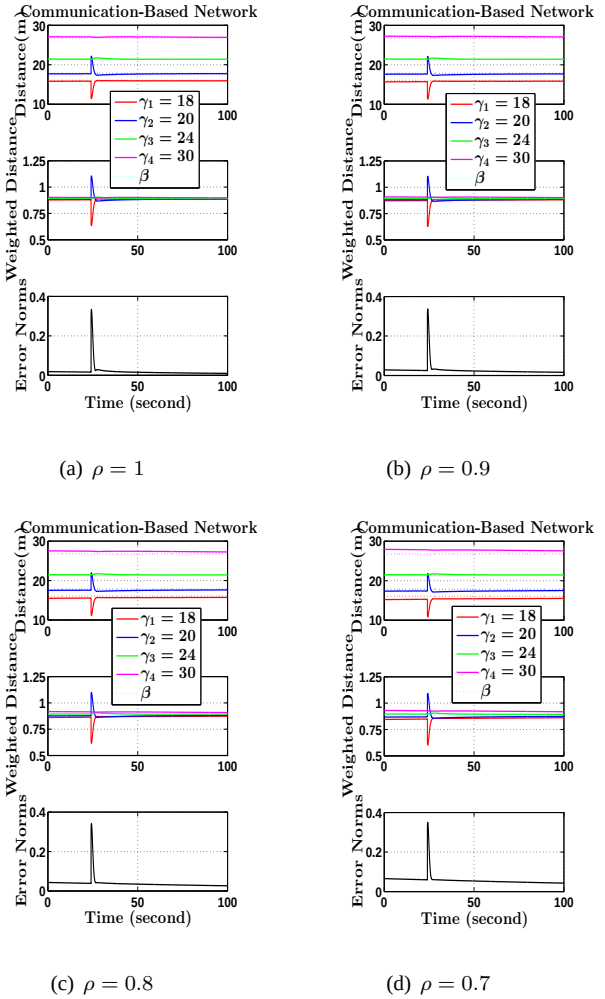

(a) $\rho = 1$ (b) $\rho = 0.9$

(c) $\rho = 0.8$ (d) $\rho = 0.7$

Fig. 9. Platoon control performance with vehicle dynamics in communication erasure channels and relatively slow local controllers

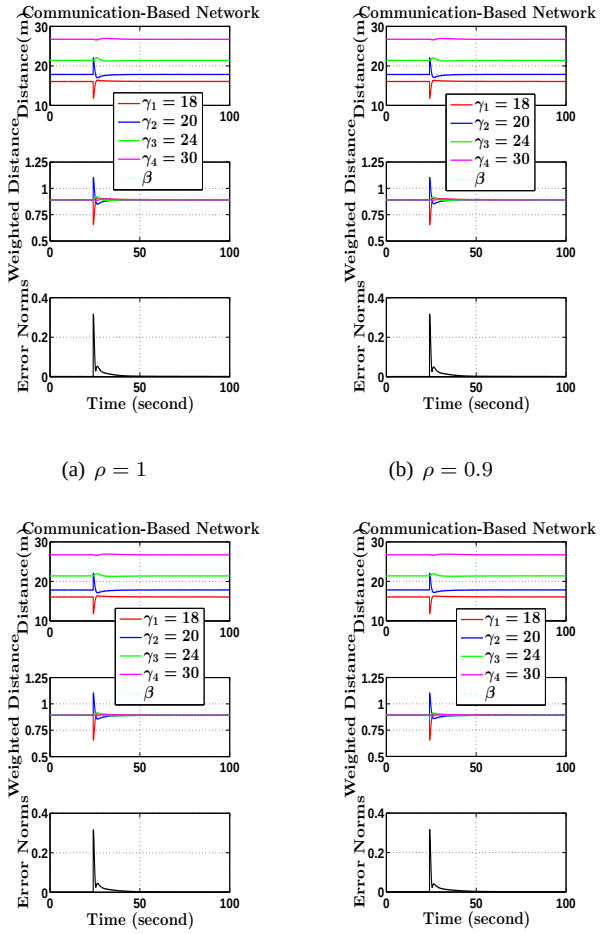

(a) $\rho = 1$ (b) $\rho = 0.9$

(c) $\rho = 0.8$ (d) $\rho = 0.7$

Fig. 10. Platoon control performance with vehicle dynamics in communication erasure channels and more aggressive local controllers.

from a platoon formation, suppose that a sudden braking of the leading vehicle results in a sudden distance change in d_1 by 4m. This disturbance causes initially a large deviation of the platoon formation.. In comparison to Fig. 9, the platoon control achieves a faster convergence. In the case of more aggressive local controllers $p = 1.4$, the weighted distances converge faster to the constant β no matter what the value of packet delivery ratio ρ is.

Finally, we evaluate the impact of the communication erasure channels on the platoon control z. In order to analyze the impact, the commonly used criterion is the weighted consensus errors. From Fig. 11 and Table IV, we have an empirical evidence to conclude that the errors converge faster if the packet delivery ratio ρ is higher. Furthermore, consensus errors converge to 0 more rapidly when more aggressive local controllers $p = 1.4$ are used.

Example 6.3: In this example, we study the impact of vehicle control in a more realistic scenario: in lieu of the model in Examples 6.1 and 6.2, we now consider a Markov chain model. For illustration, the transition matrix P of the Markov chain $\{\theta_n\}$ is the same as the one in Example 5.3.

Fig. 12 shows platoon control performances with different

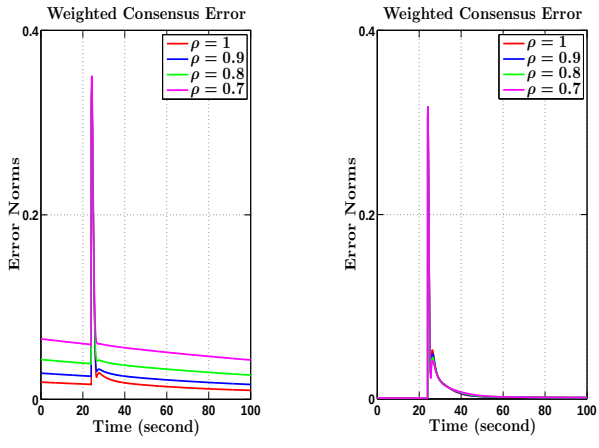

(a) $p = 1$ (b) $p = 1.4$

Fig. 11. Evolution of Weighted consensus error obtained from simulation based on 4 different choices of ρ and different choices of local controllers p.

TABLE IV
COMPARISON OF WEIGHTED CONSENSUS ERRORS OBTAINED FROM SIMULATION BASED ON 4 DIFFERENT CHOICES OF ρ AND DIFFERENT CHOICES OF LOCAL CONTROLLERS p.

Time	$p=1$			
	$\rho=1$	$\rho=0.9$	$\rho=0.8$	$\rho=0.7$
20	0.01657	0.02553	0.03930	0.06037
40	0.01782	0.02505	0.03696	0.05592
60	0.01379	0.02108	0.03270	0.05094
80	0.01137	0.01827	0.02922	0.04657
100	0.00971	0.01609	0.02632	0.04265
Time	$p=1.4$			
	$\rho=1$	$\rho=0.9$	$\rho=0.8$	$\rho=0.7$
20	0.000977	0.001031	0.001017	0.001064
40	0.005547	0.006109	0.006826	0.007445
60	0.002068	0.002145	0.002165	0.002252
80	0.001572	0.001617	0.001618	0.001706
100	0.001314	0.001338	0.001374	0.001535

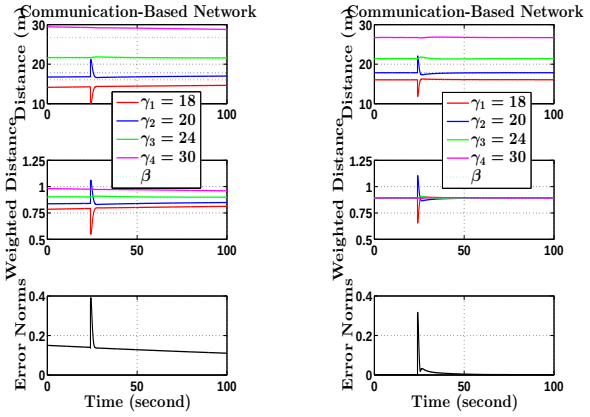

(a) $p = 1$ (b) $p = 1.4$

Fig. 12. Platoon control performance with vehicle dynamics in Markovian communication erasure channel based on different choices of local controllers p.

local controllers p. As expected, all these results clearly illustrate that the performance of the platoon control in the case of more aggressive controllers $p = 1.4$ outperforms the ones in the low-gain controllers $p = 1$.

Let us remark that with the specific transition matrix as in Example 5.3 the platoon control in Fig. 9 achieve a faster convergence then the one in Fig. 12. However, in comparison to Fig. 10, the platoon control trajectories converge fast in both i.i.d case and Markov chain case. These results clearly show that with the more aggressive controllers $p = 1.4$ the algorithm provides better performance in both i.i.d and Markovian channels.

VII. CONCLUSION

In this paper, we have addressed the problem of communication erasure channels on control performance of connected and automated vehicles under the weighted and constrained consensus framework. Markov chain models are used to represent switching network topologies resulted from channel erasures. Under some traditional assumptions on the ergodicity of the Markov chains, by using techniques from stochastic approximation, desired convergence properties of the proposed control algorithm are established. We have also investigated the impact of communication erasure channels on the interactions between consensus decision on the cyber space and vehicle control in the physical space. Our findings are verified by various numerical simulations. Not only do the numerical simulations demonstrate that communication erasure channels have significant impact on vehicle platoon performance but also they highlight robustness of vehicle platoon control under the WCCCA.

One important direction of platoon control is to consider more comprehensive two-dimensional movements. We have recently introduced a new framework to deal with similar problems for pedestrian movements [42]. In this framework, two-dimensional movements are modeled by a virtual m lane scenario in which a two-time-scale model is introduced. The framework models the in-lane movements as a platoon-type multi-agent dynamic system in continuous time, and lane changes are Markov chains. Convergence properties have been established.

REFERENCES

[1] N. Alam and A.G. Dempster. Cooperative positioning for vehicular networks: facts and future. *IEEE Transactions on Intelligent Transportation Systems*, 14(4). pp. 1708-1717, 2013.

[2] R. O'brien, P. Iglesias, and T. Urban. Vehicle lateral control for automated highway systems. *IEEE Transactions on Control Systems Technology*, 4(3), pp. 266-273, 1996.

[3] J.K. Hedrick, D. Mcmahnon, and D. Swaroop. Vehicle modeling and control for automated highway systems. *California Partners for Advanced Transit and Highways (PATH)*, 1993.

[4] R. Rajamani, H.-S. Tan, B.K. Law, and W.-B. Zhang. Demonstration of integrated longitudinal and lateral control for the operation of automated vehicles in platoons. *IEEE Transactions on Control Systems Technology*, 8(4), pp. 695-708, 2000.

[5] A. Ghasemi, R. Kazemi, S. Azadi, Stable Decentralized Control of Platoon of Vehicles with Heterogeneous Information Feedback, *IEEE Transactions on Vehicular Technology*, pp. 4299 4308, 2013.

[6] D. Swaroop and J. Hedrick. String stability of interconnected systems. *IEEE Transactions on Automatic Control*, 41(3), pp. 349-357, 1996.

[7] C.-Y. Liang and H. Peng. String stability analysis of adaptive cruise controlled vehicles. *JSME International Journal Series C*, 43(3), pp. 671-677, 2000.

[8] L. Xiao, F. Gao. Practical string stability of platoon of adaptive cruise control vehicles, *IEEE Transactions on Intelligent Transportation Systems*, pp. 1184-1194, 2011.

[9] H.C.-H. Hsu and A. Liu. Kinematic design for platoon-lane-change maneuvers. *IEEE Transactions on Intelligent Transportation Systems*, 9(1), pp. 185-190, 2008.

[10] Ge Guo, Wei Yue. Autonomous Platoon Control Allowing Range-Limited Sensors. *IEEE Transactions on Vehicular Technology*, vol. 61, no. 7, pp. 2901-2912, 2012.

[11] S.-B. Choi and J. Hedrick. Vehicle longitudinal control using an adaptive observer for automated highway systems. In *Proceedings of the 1995 American Control Conference*, volume 5, pp. 3106-3110, 1995.

[12] Y. Zheng, S. E. Li, K.Q. Li, Francesco Borrelli, and J. Karl Hedrick. Distributed Model Predictive Control for Heterogeneous Vehicle Platoons under Unidirectional Topologies. *IEEE Trans. Control Syst. Tech.*, vol. 25, issue 3, 2017, pp. 899-910.

[13] D. Swaroop, J. K. Hedrick, C. C. Chien, et al. A comparision of spacing and headway control laws for automatically controlled vehicles1. *Vehicle System Dynamics*, pp. 597-625, 1994.

[14] S. E. Li, Y. Zheng, K.Q. Li , J.Q. Wang, An Overview of Vehicular Platoon Control under the Four-component Framework, in *IEEE proceedings of 26th Intelligent Vehicle Symposium*, pp. 286-291, 2015.

[15] J. Turner. *Automotive Sensors*. Momentum Press, 2009.

[16] A. Lapidoth. The performance of convolutional codes on the block erasure channel using various finite interleaving techniques. *IEEE Transactions on Information Theory*, 40(5), pp. 1459-1473, 1994.

[17] X. Yin, X. Ma, and K.S. Trivedi. An interacting stochastic models approach for the performance evaluation of DSRC vehicular safety communication. *IEEE Transactions on Computers*, 62(5), pp. 873-885, 2013.

[18] K.A. Hafeez, L.Zhao, B. Ma, and J.W. Mark. Performance analysis and enhancement of the dsrc for vanet's safety applications. *IEEE Transactions on Vehicular Technology*, 62(7), pp. 3069-3083, 2013.

[19] J. Freudenberg and R.H. Middleton. Feedback control performance over a noisy communication channel. In *IEEE Information Theory Workshop, 2008*, pp. 232-236, Porto Portugal, May 2008.

[20] R. Luck and A. Ray. Experimental verification of a delay compensation algorithm for integrated communication and control systems. *International Journal of Control*, 59(6), pp. 1357-1372, 1994.

[21] L. Moreau. Stability of multiagent systems with time-dependent communication links. *IEEE Transactions on Automatic Control*, 50(2), pp. 169-182, 2005.

[22] A.J. Rojas, J.H. Braslavsky, and R.H. Middleton. Fundamental limitations in control over a communication channel. *Automatica*, 44(12), pp. 3147-3151, 2008.

[23] L. Xu, L.Y. Wang, G. Yin, and H. Zhang. Communication information structures and contents for enhanced safety of highway vehicle platoons. *IEEE Transactions on Vehicular Technology*, 63(9), pp. 4206-4220, 2014.

[24] L. Xu, L.Y. Wang, G. Yin, and H. Zhang. Impact of communication erasure channels on the safety of highway vehicle platoons. *IEEE Transactions on Intelligent Transportation Systems*, 16(3), pp. 1456-1468, 2015.

[25] T. Richardson and R. Urbanke. *Modern Coding Theory*. Cambridge University Press, 2008.

[26] B. Fritchman. A binary channel characterization using partitioned Markov chains. *IEEE Transactions on Information Theory*, 13-2, pp. 221-227, April 1967.

[27] H.S. Wang and N. Moayeri, Finite-state Markov channel-a useful model for radio communication channels, *IEEE Transactions on Vehicular Technology*, 44-1, pp. 163 - 171, Feb 1995.

[28] Q.Q. Zhang and S.A. Kassam, Finite-state Markov model for Rayleigh fading channels, *IEEE Transactions on Communications*, 47-11, pp. 1688-1692, Nov 1999.

[29] F. Babich and G. Lombardi. A Markov model for the mobile propagation channel. *IEEE Transactions on Vehicular Technology*, 49-1, pp. 63-73, Jan 2000.

[30] L. Wang, A. Syed, G. Yin, A. Pandya, and H. Zhang. Control of vehicle platoons for highway safety and efficient utility: Consensus with communications and vehicle dynamics. *Journal of Systems Science and Complexity*, 27(4), pp. 605-631, 2014.

[31] G. Yin, Y. Sun, and L.Y. Wang. Asymptotic properties of consensus-type algorithms for networked systems with regime-switching topologies. *Automatica*, 47(7), pp. 1366-1378, 2011.

[32] A. Guillen, I. Fabregas, and G. Caire. Coded modulation in the blockfading channel: Code construction and coding theorems. *IEEE Transactions on Information Theory*, 52(1), pp. 91-114, 2006.

[33] R. Knopp and P.A. Humblet. On coding for block fading channels. *IEEE Transactions on Information Theory*, 46(1), pp. 189-205, 2000.

[34] D.J. Costello Jr, A.E. Pusane, S. Bates, and K. S. Zigangirov. A comparison between ldpc block and convolutional codes. In *Proc. Information Theory and Applications Workshop, San Diego, CA, USA*, pp. 6-10, 2006.

[35] H. Kushner and G. Yin. *Stochastic Approximation and Recursive Algorithms and Applications*, Springer, 2003.

[36] S. Karlin and H.M. Taylor. A First Course in Stochastic Processes. *Academic Press Inc.*, New York, ISBN, 2nd edition, 1975.

[37] G. Yin, L.Y. Wang, Y. Sun, D. Casbeer, R. Holsapple, and D. Kingston. Asymptotic optimality for consensus-type stochastic approximation algorithms using iterate averaging. *Journal of Control Theory and Applications*, 11(1), pp. 1-9, 2013.

[38] G. Yin. On extensions of polyak's averaging approach to stochastic approximation. *Stochastics*, 36(3-4), pp. 245-264, 1991.

[39] G. Yin and K. Yin. Asymptotically optimal rate of convergence of smoothed stochastic recursive algorithms. *Stochastics*, 47(1-2), pp. 21-46, 1994.

[40] R.A. Horn and C.R. Johnson. Matrix Analysis. *Cambridge University Press*, 2012.

[41] B. Kuo. Automatic Control Systems. *John Wiley & Sons*, 8th edition, 2002.

[42] Qianling Wang, Hairong Dong, Bin Ning, Le Yi Wang, George Yin, Two-time-scale hybrid traffic models for pedestrian crowds, *IEEE Transactions on Intelligent Transportation Systems*, accepted in 2017.

Thu Nguyen received the B.Sc in Mathematics and Computer Sciences from the University of Sciences HCM VNU, Vietnam, in 2008 and the M.Sc in Applied Mathematics from University of Orléans, France, in 2010. She completed her Ph.D degree in Statistical Signal Processing at Lille 1 University - Science and Technology, France, in 2014. She is currently pursuing a Ph.D. in applied mathematics at Wayne State University. Her research interests are in the areas of Monte Carlo methods for Bayesian inference in complex and high-dimensional problems, stochastic approximation, stochastic control, applied probability and stochastic processes.

Le Yi Wang (S'85-M'89-SM'01-F'12) received the Ph.D. degree in electrical engineering from McGill University, Montreal, Canada, in 1990. Since 1990, he has been with Wayne State University, Detroit, Michigan, where he is currently a Professor in the Department of Electrical and Computer Engineering. His research interests are in the areas of complexity and information, system identification, robust control, H-infinity optimization, time-varying systems, adaptive systems, hybrid and nonlinear systems, information processing and learning, as well as medical, automotive, communications, power systems, and computer applications of control methodologies. He was a keynote speaker in several international conferences. He serves on the IFAC Technical Committee on Modeling, Identification and Signal Processing. He was an Associate Editor of the IEEE Transactions on Automatic Control and several other journals. He was a Visiting Faculty at University of Michigan in 1996 and Visiting Faculty Fellow at University of Western Sydney in 2009 and 2013. He is a member of the Core International Expert Group at Academy of Mathematics and Systems Science, Chinese Academy of Sciences, and an International Expert Adviser at Beijing Jiao Tong University. He is a Fellow of IEEE.

George Yin (S'87-M'87-SM'96-F'02) received the B.S. degree in mathematics from the University of Delaware in 1983, and the M.S. degree in electrical engineering and the Ph.D. degree in applied mathematics from Brown University in 1987. He has been with Wayne State University since 1987. He became a Professor in 1996 and university Distinguished Professor in 2017. His research interests include stochastic processes, stochastic systems theory and applications, stochastic approximation, identification, and signal processing. He served as Co-chair for a number of conferences and served on many committees for IFAC, IEEE, and SIAM. He was Chair of the SIAM Activity Group on Control and Systems Theory, and served on the Board of Directors of the American Automatic Control Council. He is Editor-in-Chief of SIAM Journal on Control and Optimization 2018-, Associated Editor of Applied Mathematics and Optimization, and on the editorial boards of a number of other journals; he is a senior editor of IEEE Control Systems Letters. He was an Associate Editor of Automatica 1995-2011 and IEEE Transactions on Automatic Control 1994-1998. He is a Fellow of IFAC and a Fellow of SIAM.

Hongwei Zhang (S01-M07-SM13) is an associate professor of electrical and computer engineering at Iowa State University, U.S.A. His primary research interests lie in the modeling, algorithmic, and systems issues in trustworthy wireless networking for real-time cyber-physical-human systems such as those in mixed-reality, agriculture, connected and automated vehicles, smart grid, and industrial automation. He is a recipient of the NSF CAREER Award. (URL: http://www.ece.iastate.edu/ hongwei).

Shengbo Eben Li received the M.S. and Ph.D. degrees from Tsinghua University in 2006 and 2009. He worked at Stanford University, University of Michigan, and University of California Berkeley. He is currently tenured associate professor at Tsinghua University. His active research interests include intelligent vehicles and driver assistance, reinforcement learning and distributed control, optimal control and estimation, etc. He is the author of over 100 peer-reviewed journal/conference papers, and the co-inventor of over 20 Chinese patents. Dr. Li was the recipient of Best Paper Award in 2014 IEEE ITS Symposium, Best Paper Award in 14th ITS Asia Pacific Forum, National Award for Technological Invention in China (2013), Excellent Young Scholar of NSF China (2016), Young Professorship of Changjiang Scholar Program (2016). He is now the IEEE senior member, and serves as associated editor of IEEE ITSM and IEEE Trans ITS, etc

Keqiang Li obtained the M.S. and Ph.D. degrees from Chongqing University of China in 1988 and 1995 respectively and his B.Tech degree from Tsinghua University of China in 1985. Dr. Li is the Professor of Automotive Engineering at Tsinghua University. His main research areas include intelligent and connected vehicles, automotive control system, driver assistance system, vehicle dynamics and control. Currently he is leading the national key project on connected and automated vehicles in China. Dr. Li has authored about 180 journal/conference papers and is a co-inventor of over 60 patents in China and Japan. Dr. Li has served as the Fellow of Society of Automotive Engineers of China, editorial boards of International J of ITS Research and International J of Vehicle Autonomous Systems, and Chairperson of Technical Committee of CAICA. Dr. Li has been a recipient of Changjiang Scholar Program Professor, National Award for Technological Invention in China, etc.